Nonlinear vibrations and chaos in gongs and cymbals

Antoine Chaigne, Cyril Touzé, Olivier Thomas

Nonlinear vibrations and chaos in gongs and cymbals

Antoine Chaigne[1,*], Cyril Touzé[1,†] and Olivier Thomas[2,‡]

[1]*ENSTA-UME, Chemin de la Hunière, 91761 Palaiseau cedex, France*
[2]*CNAM, 2 rue Conté, 75003 Paris, France*

Abstract: This paper summarizes some results obtained in the last few years for the modeling of nonlinear vibrating instruments such as gongs and cymbals. Linear, weakly nonlinear and chaotic regimes are successively examined. A theoretical mechanical model is presented, based on the nonlinear von Kármán equations for thin shallow spherical shells. Modal projection and Nonlinear Normal Mode (NNM) formulation leads to a subset of coupled nonlinear oscillators. Current developments are aimed at using this subset for sound synthesis purpose.

Keywords: Gongs and cymbals, Nonlinear vibrations, Bifurcations, Combination of modes, Chaos

1. INTRODUCTION

Gongs and cymbals belong to the category of percussive instruments. They are sometimes denoted as "nonlinear percussion instruments," which emphasizes the fact that nonlinearity is essential in the production of sound by such sources. In normal use, the vibratory displacement is of the order of magnitude of the thickness, which induces geometrical nonlinearity. Therefore, a proper description of the phenomena has to include such nonlinear terms in the model.

Experimentations performed on these instruments for many years have shown the typical features of this nonlinear behavior: amplitude-dependent level of harmonics in the spectrum, pitch glide, bifurcations, energy exchange between modes through nonlinear coupling and chaos [1–6]. More recently, similar experiments were made on structures of simpler geometry (circular plates, shallow spherical shells) which exhibit comparable effects [7–10]. The aim of the present paper is to summarize recently observed experimental results and to assess the pertinence of a nonlinear model with quadratic geometrical nonlinearity in describing such effects.

Most experiments were conducted on real cymbals and gongs punctually excited by a sinusoidal electromagnetic force with slowly increasing (or decreasing) amplitude. The recorded punctual velocity shows bifurcations from linear to chaotic regime. Two transitions are commonly observed: the first bifurcation can be explained by energy exchange between normal modes which are strongly coupled by an internal resonance relationship. After the second transition, the velocity signal exhibits a chaotic behavior. Although the excitation signal is a pure tone, it is important to notice that the chaotic regime sounds similar to real instruments normally excited by the strong impact of a mallet.

The theoretical model is based on the von Kármán nonlinear equations for large deflections of thin shallow spherical shells. As a result of the projection of the solution on the linear modes of the structure, a set of nonlinear coupled differential equations is obtained that govern the dynamics of the problem. In these oscillator equations, the coefficients are directly connected to the geometry and elastic properties of the vibrating object. A truncation of this set of nonlinearly coupled oscillators is performed in order to investigate the essential properties of the combination of modes. Instability conditions and the threshold values for the excitation are derived from the resolution of these subsets, using the method of multiple scales. Using nonlinear normal modes (NNM), a subset composed of a limited number of equations is obtained which approximate the solution more accurately than a subset obtained from the linear modal projection [11].

2. SUMMARY OF EXPERIMENTS

In their normal use, cymbals and gongs are set into vibrations by means of a mallet impact. However, as stated in [5], the nonlinear vibrations are due to large amplitude motion and can be thus studied using sinusoidal excitation, which greatly simplifies the interpretation. In fact, one can

*e-mail: antoine.chaigne@ensta.fr
†e-mail: cyril.touze@ensta.fr
‡e-mail: olivier.thomas@cnam.fr

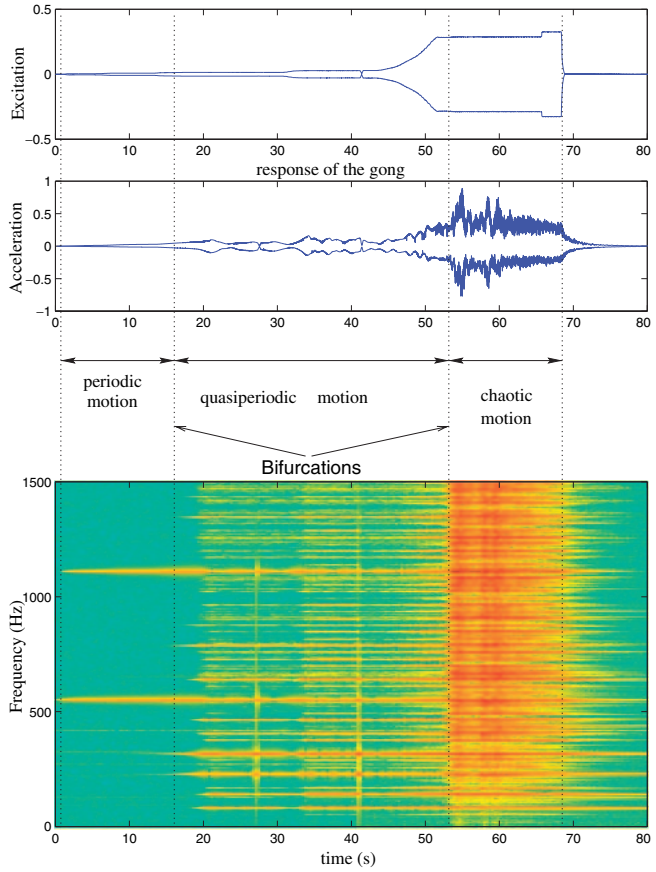

Fig. 1 Harmonic excitation of a gong with increasing force amplitude.

notice that sounds produced with strong harmonic excitation are very similar to those resulting from impulsively excited instruments.

Figure 1 shows the fundamental experiments performed on the investigated instruments and structures. The top of the figure shows the progressively increasing noncontact excitation force at frequency Ω close to one eigenfrequency of the structure. As a result, the transverse acceleration of one selected point exhibits first a periodic motion with increasing level of harmonics 2Ω, 3Ω,... A first bifurcation occurs suddenly for a given force threshold. This bifurcation is characterized by the apparition of new frequencies ω_i and ω_j whose values are governed by the following rules:

$$\begin{aligned} p\Omega &= a_i\omega_i + a_j\omega_j \\ \text{with} \quad a_i, a_j \in \mathbb{Z} \quad &\text{and} \quad |a_i| + |a_j| = 2 \end{aligned} \tag{1}$$

where p is the harmonicity order of the excitation and ω_i and ω_j are other eigenfrequencies of the structure. These rules are direct consequences of quadratic nonlinearity [12]. The first equation in (1) characterizes the phenomenon of *combination resonances*. It shows that combinations can occur under the condition that one eigenfrequency, or one of its multiple, has particular algebraic relationship with one or two other eigenfrequencies. This property is called *internal resonance*.

Between the first and second bifurcation, the motion is quasiperiodic. The spectrum is enriched by the various frequencies ω_i and ω_j, resulting from the combination rules, and by their harmonics. After the second bifurcation, the spectrum is broadband. Calculating the Lyapunov exponents in this part shows that the motion is chaotic [3] (see Section 6).

3. LINEAR ANALYSIS

As shown in Section 2 the nonlinear behavior of the structure depends on its eigenfrequencies. This imposes to investigate first its linear vibrations. The linear motion of the structure is governed by an equation of the form:

$$\mathcal{L}(w) + \ddot{w} = 0 \tag{2}$$

where w is the transverse displacement of the thin shallow structure and $\mathcal{L}(w)$ a linear operator. A free edge boundary condition is added. Eq. (2) was solved analytically for a thin shallow shell, after confirmation that the main features of nonlinear vibrations for these structures were similar to those of gongs and cymbals [7]. This equation was also solved numerically, using a Finite Element modeling, for orchestral gongs (Chinese tam-tam), for cymbals, and for spherical caps with two different curvatures, successively. This latter case, in particular, shows that the values of the eigenfrequencies are highly sensitive to small changes of curvature. In addition, the modal shapes are strongly influenced by slope discontinuities. This property was mentioned in previous studies by Fletcher [2]. Finally, the linear analysis confirms the particularity of structures with symmetry of revolution which exhibit two modes with equal eigenfrequencies under the assumption of perfect homogeneity. For spherical caps, the experiments show some slight differences in frequency due to small imperfections (suspensions, holes, local defects,...). For the Chinese tam-tam, significant differences between the frequencies of the "twin modes" are observed, due to the loss of symmetry in the structure. The exact causes of this asymmetry are not yet fully understood.

4. WEAKLY NONLINEAR REGIME

4.1. Pitch Glide

An aurally impressive effect of some relatively thick and massive gongs is the pitch glide exhibited when struck near their center. As mentioned by Fletcher [4], different effects can be observed. For a large Chinese opera gongs, whose central striking surface is flat, for example, a downward glide in pitch "by as much as three semitones" can be heard. On the other hand, smaller gongs with a pronounced curvature, glide upward.

Such properties can be related to the amplitude-

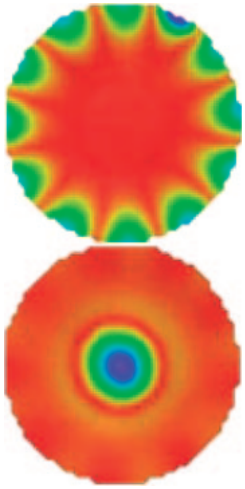

Fig. 2 Measured linear eigenmodes of the spherical cap linked by internal resonance of order two. Top: Mode (6,0) - $f = 111$ Hz; Bottom: Mode (0,1) - $f = 224$ Hz.

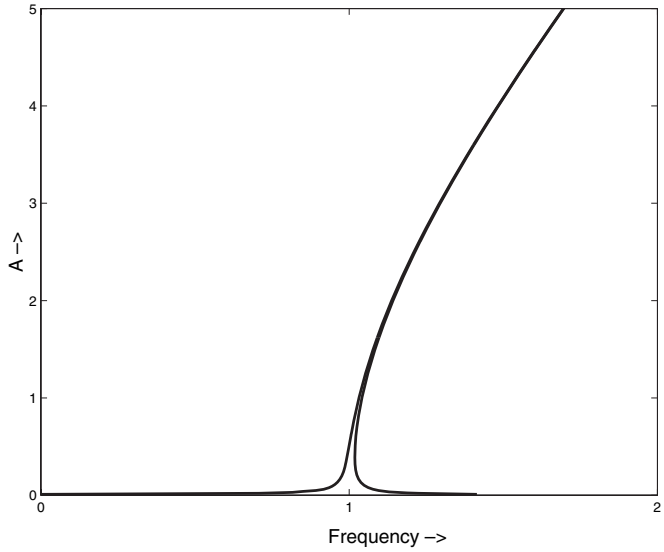

Fig. 3 Typical resonance curve for a nonlinear oscillator of the *hardening* type.

frequency curve exhibited by nonlinear oscillators of the Duffing type [12]. A non-linear oscillator shows a hardening behaviour when the resonance curve is bent to the right (direction of increasing frequencies) (see Fig. 3), which corresponds to a downward pitch glide in free vibrations, since the amplitude of the damped oscillator decreases with time. On the contrary, a softening behaviour corresponds to a resonance curve bent to the left and yields an upward pitch glide for free vibrations.

When gongs are struck at the center, the prime excited mode is the first axisymmetric mode. For flat plates, this leads to a hardening behaviour governed by cubic nonlinearity. When a curvature is present, the type of behaviour (hardening or softening) depends on the balance between quadratic and cubic terms. The transition between these two cases has been studied by Fletcher, for a single mode of simple rods systems, by Thomas *et al.* [13], and, more exhaustively, by Touzé and Thomas for shallow spherical shells [14]. In this latter paper, it is shown that increasing the curvature leads to changing the behaviour from hardening to softening. This yields, among other things, a theoretical proof for the experimental effects observed by Fletcher [4] and Rossing [15].

Notice that pitch glide occurs as long as the nonlinearity is kept relatively weak. This explains why pitch glides are frequently heard on thick gongs, but not on thin cymbals, where the crash shimmering sound is the dominant feature. These observations are in agreement with the experimental results presented below. For thin structures, nonlinear effects are present even for very small amplitude of vibration, and thus energy transfer and mode coupling phenomena usually appear before the pitch glide.

4.2. Nonperiodic Regime

The presence of new frequencies in the nonperiodic motion can be explained by a stability study performed on a finite set of nonlinearly coupled oscillators. We take here the example of a system with an internal resonance of order two. This corresponds to a three-modes subset for which we have $\omega_3 \simeq 2\omega_2 \simeq 2\omega_1$ and $\varepsilon \ll 1$. This configuration is observed on the spherical cap as the symmetric mode (0,1) forced at the center excites the twin asymmetric modes $(6,0)_a$ and $(6,0)_b$ through nonlinear coupling (see Fig. 2 and Section 5).

The solution is obtained by applying the method of multiple scales [10] to the system:

$$\begin{aligned}
&\ddot{x}_1 + {\omega_1}^2 x_1 = \varepsilon[-\beta_{13} x_1 x_3 - 2\mu_1 \dot{x}_1] \\
&\ddot{x}_2 + {\omega_2}^2 x_2 = \varepsilon[-\beta_{23} x_2 x_3 - 2\mu_2 \dot{x}_2] \\
&\ddot{x}_3 + {\omega_3}^2 x_3 = \varepsilon[-\beta_{11} {x_1}^2 - \beta_{22} {x_2}^2 - 2\mu_3 \dot{x}_3 + P\cos\Omega t]
\end{aligned} \tag{3}$$

The shell is excited at a frequency close to the asymmetric eigenfrequency, so that the forcing frequency can be written $\Omega = \omega_3 + \varepsilon\sigma_2$, where σ_2 is the external detuning parameter. The coefficients β_{13}, β_{23}, β_{12}, β_{11} and β_{22} depend on the geometry and material of the structure. The damping coefficients μ_1, μ_2 and μ_3 are generally derived from experiments [10]. Solving Eq. (3) yields solutions of the form [6]:

$$\begin{aligned}
x_1 &= a_1 \cos\left(\frac{\Omega}{2} t - \frac{\gamma_1 + \gamma_3}{2}\right) \\
x_2 &= a_2 \cos\left(\frac{\Omega}{2} t - \frac{\gamma_2 + \gamma_3}{2}\right) \\
x_3 &= a_3 \cos(\Omega t - \gamma_3)
\end{aligned} \tag{4}$$

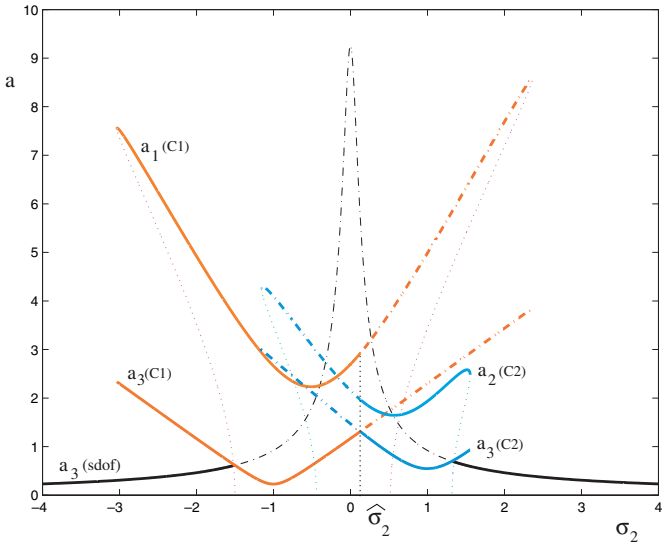

Fig. 4 Generalized stability curve for the case: $\beta_{13} = -7$, $\beta_{23} = -5$, $\beta_{11} = -3$, $\beta_{22} = -4$, $\mu_1 = \mu_3 = 0.1$, $\mu_2 = 0.2$, $P = 16$, $\omega_1 = 4$, $\omega_2 = 4.09$, $\omega_3 = 8.1$. Stable branches are plotted with solid lines, all other branches are unstable.

Figure 4 shows that, under certain conditions of both forcing amplitude and external detuning, stable subharmonics of order 2 with amplitudes a_1 and a_2 can exist.

5. NONLINEAR MECHANICAL MODEL

It is now examined how nonlinearly coupled oscillators of the form (3) can be derived from the equations of motion of a shallow free-edge spherical cap with geometrical nonlinearities. The shell is assumed to be thin so that its thickness $h \ll a$, where a is the radius of the circle corresponding to the horizontal projection of the cap. It is also supposed to be shallow, which implies $h \ll R$ where R is the radius of curvature (see Fig. 5).

5.1. Equations of Motion

The nonlinear flexural motion of thin shallow spherical shells is well described by generalized von Kármán

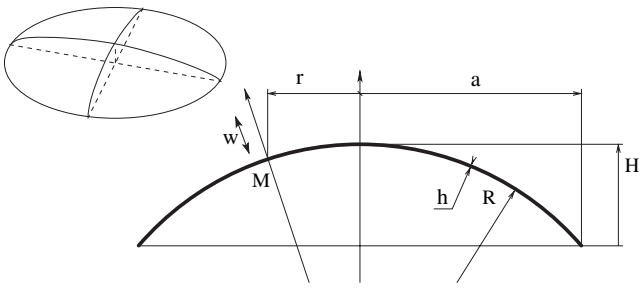

Fig. 5 Geometry of the spherical cap.

equations [8]. Normalizing the displacement with respect to the quantity h^2/a, where a is the radius of the circle corresponding to the projection of the shell onto a plane perpendicular to its axis, and h its thickness, the equations of motion can be written in the following nondimensional form:

$$\begin{aligned} \Delta^2 w + \ddot{w} &= -\varepsilon_q \Delta F + \varepsilon_c [S(w,F) - 2\mu\dot{w} + p] \\ \Delta^2 F - \frac{a^3}{Rh^2}\Delta w &= -\frac{1}{2} S(w,w) \end{aligned} \tag{5}$$

where F is the Airy stress function, S is a nonlinear operator, μ is a damping coefficient, p is the forcing pressure and R the radius of curvature. The quadratic (ε_q) and cubic (ε_c) parameters are given by:

$$\varepsilon_q = 12(1-\nu^2)\frac{a}{R}; \quad \varepsilon_c = 12(1-\nu^2)\frac{h^2}{a^2} \tag{6}$$

where ν is the Poisson's ratio. For common geometries of thin shallow spherical shells, cymbals and gongs, we have $\varepsilon_c \ll \varepsilon_q$. Projection of Eq. (5) onto the eigenmodes of the structures with free edge yields the set of differential equations for the modal participation factors $q_i(t)$:

$$\begin{aligned} \ddot{q}_i + {\omega_i}^2 q_i = &-\varepsilon_c \sum_j \sum_k \sum_l \gamma^i_{jkl}\, q_j q_k q_l \\ &+ \varepsilon_q \left[-\sum_j \sum_k \beta^i_{jk}\, q_j q_k - 2\mu_i \dot{q}_i + P_i(t) \right] \end{aligned} \tag{7}$$

Explicit expressions of the coefficients β^i_{jk} and γ^i_{jkl} can be found in [8].

For the case presented in Fig. (2), we can assume that the nonlinear coupling only involves the asymmetric modes (6,0) and the symmetric mode (0,1), so that we can truncate Eq. (7) and write the approximation:

$$\begin{aligned} w(r,\theta,t) \approx\ & \Phi_{60}(r)[q_1(t)\cos 6\theta + q_2(t)\sin 6\theta] \\ &+ \Phi_{01}(r) q_3(t) \end{aligned} \tag{8}$$

where q_1 and q_2 are the time histories of the two quadrature configurations of the asymmetric modes (6,0). This truncation yields finally:

$$\begin{aligned} \ddot{q}_1 + {\omega_1}^2 q_1 &= \varepsilon_q[-\beta_{13} q_1 q_3 - 2\mu_1 \dot{q}_1] \\ \ddot{q}_2 + {\omega_2}^2 q_2 &= \varepsilon_q[-\beta_{23} q_2 q_3 - 2\mu_2 \dot{q}_2] \\ \ddot{q}_3 + {\omega_3}^2 q_3 &= \varepsilon_q[-\beta_{11} {q_1}^2 - \beta_{22} {q_2}^2 - 2\mu_3 \dot{q}_3 + P_3(t)] \end{aligned} \tag{9}$$

where the cubic terms have been neglected, according to Eq. (6).

Further simplifications are obtained by the use of NNM (see below). In practice, experiments show that the previous equations remain valid for $\|w\| \sim h$ and $R \sim a$, even if some of the nondimensional perturbating terms are not kept small compared to unity.

5.2. Nonlinear Normal Modes (NNM) Formulation

NNM theory was developed in order to extend some of the properties of the linear normal modes to nonlinear systems. The leading idea is to decouple the nonlinear oscillators, in order to appropriately truncate the infinite series of differential equations derived from the nonlinear Partial Differential Equations that govern the motion. A NNM is defined as an invariant manifold in phase space, i.e. as a two-dimensional surface that is tangent to the linear modal eigenspace at the equilibrium point. As written in [16], the term "invariant" indicates that "any motion initiated on the manifold will remain on it for all time." In the context of sound synthesis, NNM are used for simplifying the dynamical system while keeping the essential features of the motion: hardening/softening behavior, dependence of mode shape with amplitude. In practice, the reduction is obtained through nonlinear change of coordinates based on normal form theory [11]. From a physical point of view, this approach shows that the nonlinear dynamics is governed by a small number of *active* modes. This means that only a limited number of nonlinear oscillators are strongly coupled, and thus it is possible to reduce the dimension of Eq. (7) without affecting the global energy flow through the oscillators. In our case, the number of *active* modes is generally small (5 to 10 oscillators). Time-domain simulations performed with such a projection allows to reproduce the first bifurcation with great accuracy. Simulation of the second bifurcation is currently investigated.

6. CHAOS

6.1. Phase Space

After the second bifurcation (see Fig. 1), the recorded vibratory signal exhibits a wideband spectrum where one cannot easily distinguish discrete frequency peaks anymore (see Fig. 6). It turns out that the Fourier analysis is not sufficient here for describing the dynamics of the system and one has to use other tools.

Phase space analysis is among the most efficient method for gaining insight on the dynamics of nonlinear systems. For a given time series $s(t)$, a state space trajectory is obtained through displaying of the locus of points with coordinates $(s(t), s(t+T))$ where T is a time delay whose appropriate selection will not be discussed further here [17].

As the driving amplitude is kept small (case 1), Fig. 6 shows that the space trajectory takes the form of a closed curve. With increasing amplitudes, typical foldings are observed which indicate a possible route to chaos (case 2). After the second bifurcation, the trajectory takes the form of a blurred structure (case 3). Our goal here, is to show how we can extract some invariants from this structure that could help in characterizing and quantifying the signal.

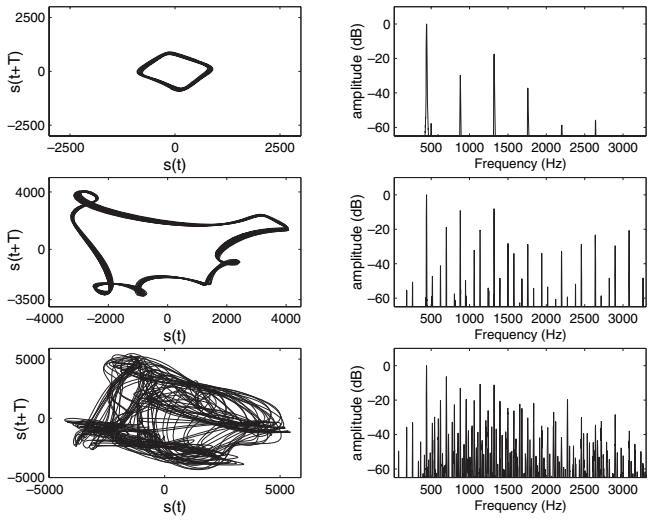

Fig. 6 Cymbal vibration. Left column: Phase space; Right column: Fourier spectrum. Top (case 1): quasi-linear regime. Middle (case 2): weakly nonlinear regime. Bottom: (case 3) chaotic regime.

6.2. Low-Dimensional Deterministic Process

The erratic structure of the signal in case 3 could incite us to think of a random process. In fact, a random process has the property that portions of extracted time series are uncorrelated. Therefore, one interesting method is to calculate a correlation dimension on gong or cymbal vibrations in order to see whether it is a random process or not. To achieve this, we start by composing vectors of the form:

$$\begin{aligned} &\boldsymbol{y}(n) = [s(n), s(n+T), \ldots, s(n+(d_E-1)T)] \\ &\text{with} \quad n = 1, \ldots, N-(d_E-1)T \end{aligned} \tag{10}$$

where $s(n)$ is the sampled version of $s(t)$ of length N, and d_E is a so-called *embedding dimension*.

The *correlation dimension* d_c is derived from the computation of a correlation integral $C(\varepsilon)$ defined as the number of points in the phase space whose mutual distance is less than a given value ε:

$$C(\varepsilon) = \frac{1}{N(N-1)} \sum_{i \neq j} H(\varepsilon - \|\boldsymbol{y}(i) - \boldsymbol{y}(j)\|) \tag{11}$$

where H is the Heaviside function and $\|.\|$ is the norm in the $\boldsymbol{y}$-vector space.

It has been shown by Grassberger and Procaccia that $C(\varepsilon) \approx \varepsilon^{d_c}$ [18]. In practice, the procedure thus consists in computing $d_c = \ln C(\varepsilon)/\ln \varepsilon$ for increasing values of the embedding dimension d_E.

Figure 7 shows d_c as a function of d_E for 4 different conditions of punctual harmonic excitation on a crash cymbal. In each case, one can see that d_c tends asymptotically to a finite value as d_E increases. These results tend to prove that the dynamics of the instrument is governed by a

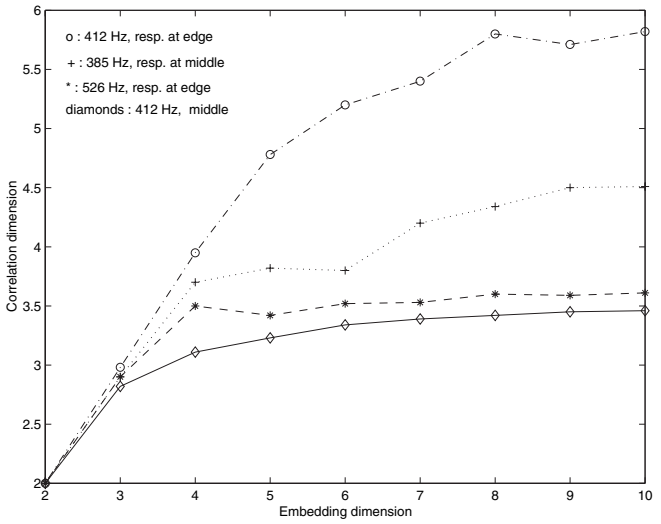

Fig. 7 Correlation dimension d_c of some vibration recordings of a harmonically excited cymbal as a function of the embedding dimension d_E.

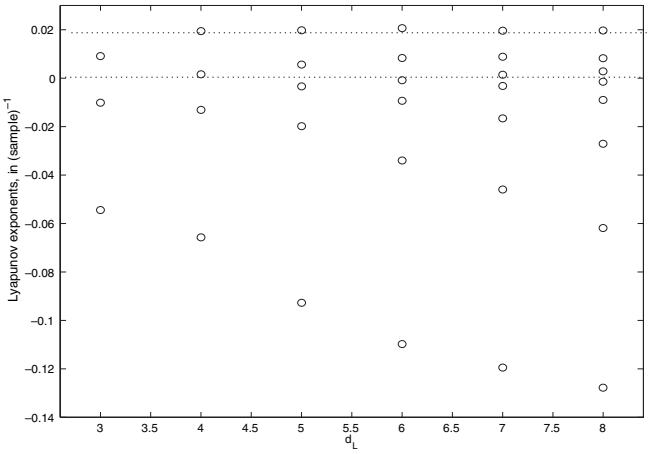

Fig. 8 Lyapunov exponents estimated from the analysis of a cymbal vibration signal. Notice the convergence to a positive exponent $\lambda = 0.02$.

finite number of degrees of freedom. Similar results are obtained in the case of gongs. In the case of a random process, d_c would have tend to infinity with increasing d_E.

6.3. Lyapunov Exponent

A chaotic system is characterized by its sensitivity to initial conditions. As a consequence, small differences in these conditions can yield very different time-evolutions of the system. In the phase space, these evolutions are seen as diverging trajectories with time. Therefore, an appropriate method for detecting and quantifying chaos is to find a measure of this divergence. For a chaotic system, the evolution with time of the distance between two points in the phase space is found to be exponential of the form $e^{\lambda t}$ where the rate $\lambda > 0$ is the *Lyapunov exponent*.

Lyapunov exponents were computed for cymbal vibrations [3]. Is has been found (see Fig. 8) that, with increasing dimensions d_L of the data vectors, at least one exponent is positive and that its value converges to a constant value. For experimental signals, the analysis often yields other exponents (positive or negative), and the selection of real and spurious exponents is a rather delicate task. One important issue to remind is that the largest exponent is the most reliable, since this exponent governs the divergence.

7. SUMMARY AND CONCLUSION

In this paper, the nature of nonlinear coupling that leads to the particular sounds of cymbals and gongs has been described, by analogy with the similar behavior of thin shallow spherical shells. The same method can be now applied to more complex geometries, though, in this case, the coupling coefficients, which depend on the modal shapes, have to be computed numerically. Is has been shown, both theoretically and experimentally, that the energy transfer between modes is a consequence of quadratic nonlinearity due to curvature of the shell and is fully governed by frequency rules. The mechanical theory also shows that instability can occur with only a limited number of degrees of freedom, which is confirmed by an estimation of the dimension obtained from nonlinear signal analysis on cymbals and gongs. Finally, the computation of Lyapunov exponents shows that the dynamics obtained in case of strong excitation is chaotic. Current development are aimed at obtaining relevant synthetic sounds from the numerical resolution of a small number of coupled nonlinear oscillators.

REFERENCES

[1] T. D. Rossing, *Science of Percussion Instruments* (World Scientific, Singapore, 2000).

[2] N. H. Fletcher, "The nonlinear physics of musical instruments," *Rep. Prog. Phys.*, **62**, 723–764 (1999).

[3] C. Touzé and A. Chaigne, "Lyapunov exponents from experimental time series: application to cymbal vibrations," *Acustica - Acta Acustica*, **86**, 557–567 (2000).

[4] N. H. Fletcher, "Nonlinear frequency shifts in quasi-spherical-caps shells: Pitch glide in Chinese gongs," *J. Acoust. Soc. Am.*, **78**, 2069–2073 (1985).

[5] K. A. Legge and N. H. Fletcher, "Nonlinearity, chaos, and the sound of shallow gongs," *J. Acoust. Soc. Am.*, **86**, 2439–2443 (1989).

[6] A. Chaigne, C. Touzé and O. Thomas, "Nonlinear axisymmetric vibrations of gongs," *Proc. Int. Symp. Mus. Acoust.*, Perugia, Vol. 1, pp. 147–152 (2001).

[7] A. Chaigne, M. Fontaine, O. Thomas, M. Ferré and C. Touzé, "Vibrations of shallow spherical shells and gongs: A comparative study," *Proc. Forum Acusticum*, Sevilla, Mus-06-006-IP (2002).

[8] O. Thomas, C. Touzé and A. Chaigne, "Nonlinear vibrations of free-edge thin spherical shells: modal interaction rules and 1:1:2 internal resonance," *Int. J. Solids Struct.*, **42**, 3339–3373

(2005).
[9] O. Thomas, E. Luminais and C. Touzé, “Nonlinear modal interactions in free-edge thin spherical shells: Measurements of a 1:1:2 internal resonance,” *3rd MIT Conf. Computational Fluid and Solid Mechanics*, Boston (2005).
[10] O. Thomas, C. Touzé and A. Chaigne, “Asymmetric non-linear forced vibrations of free-edge circular plates, Part II: experiments,” *J. Sound Vib.*, **265**, 1075–1101 (2003).
[11] C. Touzé, O. Thomas and A. Chaigne, “Hardening-softening behaviour in non-linear oscillations of structural systems using nonlinear normal modes,” *J. Sound Vib.*, **273**, 77–101 (2004).
[12] A. H. Nayfeh and D. T. Mook, *Nonlinear Oscillations* (Wiley, New York, 1979).
[13] O. Thomas, C. Touzé and A. Chaigne, “Non-linear behaviour of gongs through the dynamics of simple rods systems,” *Proc. Int. Symp. Mus. Acoust.*, Perugia (2001).
[14] C. Touzé and O. Thomas, “Nonlinear behavior of free-edge shallow spherical shells: Effect of the geometry,” *Int. J. Nonlinear Mech.* (submitted).
[15] T. D. Rossing and N. H. Fletcher, “Nonlinear vibrations in plates and gongs,” *J. Acoust. Soc. Am.*, **73**, 345–351 (1983).
[16] N. Boivin, C. Pierre and S. W. Shaw, “Nonlinear normal modes, invariance and modal dynamics approximations of nonlinear systems,” *Nonlinear Dyn.*, **8**, 315–346 (1995).
[17] H. Kantz and T. Schreiber, *Nonlinear Time Series Analysis*, Cambridge Nonlinear Sciences Series, Vol. 7 (Cambridge University Press, Cambridge, 1997).
[18] P. Grassberger and I. Procaccia, “Measuring the strangeness of strange attractors,” *Physica D*, **9**, 189–208 (1983).